

Nonlinear Dynamics of Optically Excited Chiral Nano-Spheroid in a Stationary Fluid

Tomer Berghaus⁽¹⁾, Oded Gottlieb⁽²⁾, Touvia Miloh⁽¹⁾ and Gregory Ya. Slepyan⁽³⁾

(1) School of Mechanical Engineering, Tel Aviv University, Tel Aviv 69978, t.berghaus@gmail.com, miloh@tauex.tau.ac.il Israel

(2) Faculty of Mechanical Engineering, Technion - Israel Institute of Technology, Haifa, 3200003, oded@me.technion.ac.il Israel

(3) School of Electrical Engineering, Tel Aviv University, Tel Aviv 69978, gregory_slepyan@yahoo.com Israel

Abstract – We investigate the nonlinear mechanical motion of a chiral nano-particle suspended in stationary fluid induced by a linearly polarized electromagnetic field with a rotating polarization axis. Our analysis makes use of the time-averaged optical torque, which yields a set of three nonlinear equations for the angular velocities of the 3D rotating chiral particle in terms of its time-dependent Euler angles. The effect of electromagnetic chirality dramatically changes the qualitative behavior of the optical torque. It is also shown that chirality manifests itself in the non-invariance of the particle optical torque with respect to the direction of rotation of light polarization. In order to preserve the invariant behavior, a chiral duality condition must be enforced. Some relevant experimental observations and few practical applications of predicted effect are also mentioned and discussed.

Index terms – Optical torque; Chirality; Euler angles; Rotating linear polarization.

I. INTRODUCTION

Controlling the optical torque (OT) acting on trapped nanoparticles (known as optical tweezers) is essential for different applications in nano-optics, biophysics and biotechnology [1], among them the rotation of living cells [2,3], implementation of motor proteins [2,3] and microscopic machines [4-6] have been demonstrated. The rotation of nanoparticles may be induced via scattering or absorbance of light, and one of the principles underlying the application and control of the OT acting on nanoparticles, is the use of wave-plates that rotate the direction of a linear polarized light impinging on an asymmetric nanorod suspended in a nanofluid [6]. Such apparatus produces a nonlinear mechanical motion and enables its effective control, for example by means of the “flip-back” effect [6]. In angular optical tweezers, the most commonly employed trapping particle thus far is a quartz cylinder. Crystalline quartz has an anisotropic electric susceptibility, such that the extraordinary axis of the crystal is more easily polarized than the ordinary axes. The cylinder is designed to have its extraordinary axis perpendicular to its cylindrical axis and one of its ends chemically functionalized for attachment to a biological molecule of interest. Once the cylinder is trapped,

its cylindrical axis orients along the direction of light propagation as a result of shape anisotropy i.e. experience an optical torque [7].

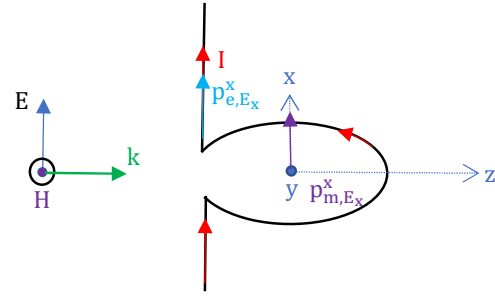


Fig.1. Deplore response of a metaparticle to an impinging EM excitation.

The advent of anisotropic and chiral materials opens a novel way for implementing OT [8-14] techniques. An object is defined to be chiral, if it is impossible to transform it onto its mirror image by rotation or translation [15]. Such asymmetry is the reason for the different response of an object with respect to opposite helicity of the incident electromagnetic wave. In Fig.1 the deplore response of a metaparticle, so called twisted- Ω , is presented. An x -directed electromagnetic (EM) excitation induces an x -directed electric dipole moment p_{e,E_x}^x on the straight section of the particle, which corresponds to the polarizability tensor component α_{ee}^{xx} and the current associated with this dipole moment, I , flows in the loop section from current continuity. However, given the 90° twist of the loop, this current now gives rise to the x -directed magnetic dipole moment p_{m,E_x}^x which corresponds to α_{me}^{xx} . Note that if the angle of the loop twist were not exactly 90° , then the induced magnetic moment would be tilted, which would introduce an off-axis contributions to the response. Therefore, chirality is a dual condition. It means that elements embedded in a host medium with a given chirality, can be used to manifest -at the nanoscale-the transition between linear to non-linear regimes and vice versa. Such phenomena can be applied in nontraditional applications [16]. The recent progress in nanotechnologies have made it possible to create new types

of chiral materials (e.g., carbon nanotubes [16] and plasmonic nanohelices [17]) with tailored properties for specific optomechanical applications. Among the promising nanotechnological applications, we can highlight modern activities such as torque sensing [18], using, for example, photo actuators and motors [17].

The remarkable properties of OT are due to the synthesis of different concepts. The main part of theoretical models of OT with chiral objects and their experimental implementations [8-14] are based on the circular polarized waves.

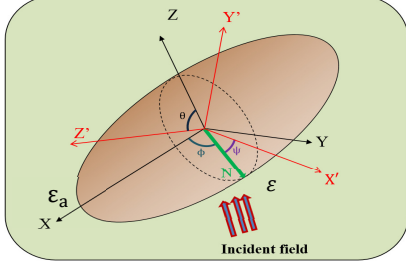


Fig.2. Rotating chiral Gold spheroid suspended in stationary fluid excited by the plane wave $\mathbf{E} = \mathbf{E}_0 e^{-i\omega t} \hat{z}$. X, Y, Z is Cartesian lab system, X', Y', Z' Cartesian rotating system and ϕ, ψ, θ Euler angles; N is the nodal line. The permittivity of the spheroid $\epsilon = (-112.41 + 20.55i)\epsilon_0$, Permittivity of liquid $\epsilon_a = 1.78\epsilon_0$ (water). The dimensions of the spheroid are: $a_x = 2500\text{nm}$, $a_z = a_y = 250\text{nm}$ and the wavelength and amplitude of the impinging plane wave are 1300nm and 10^5V/m , respectively. The relative permeability between the spheroid and its surroundings is taken as unity.

The presented study opens the path towards controlling the manner in which angular momentum is transformed to a chiral object suspended in a stationary fluid. The theory of such process is the subject of this paper, and may be considered as a generalization of the model [6] (OT of the non-chiral dielectric particle by the rotated linearly polarized light). The main result of our paper is the transformation of electromagnetic chirality to the special asymmetry of OT acting on a nanospheroid.

II. MODEL

We consider a nanospheroid suspended in stationary fluid. Under real experimental conditions [6], the moment of inertia \mathbf{I} of the object is extremely small and as a result inertia term can be ignored with respect to electromagnetic, and viscous forcing. We assume that all axes lengths of the spheroid are small compared with the exciting wavelength. Under these assumptions, the Rayleigh approximation is implemented for the description of light scattering [22] [23] [24]. The dipolar description of a small chiral object, such as a chiral nanoparticle or a chiral molecule, corresponds to a coupled system of induced electric and magnetic dipole moments. The electromagnetic behavior of a linear time-invariant (LTI) medium, can generally be expressed by the Maxwell equations with the following constitutive relations

$$\mathbf{D} = \bar{\epsilon}\mathbf{E} + \bar{\xi}\mathbf{H} \quad (1)$$

$$\mathbf{B} = \bar{\zeta}\mathbf{E} + \bar{\mu}\mathbf{H} \quad (2)$$

where $\bar{\epsilon}, \bar{\mu}, \bar{\xi}$ denote the permittivity, permeability, and magnetic-to-electric coupling dyadic tensors respectively. One particular example for which the tensors $\bar{\epsilon}, \bar{\mu}, \bar{\xi}$ and $\bar{\zeta}$ reduce to the diagonal tensors $\bar{\epsilon}\mathbf{I}, \bar{\mu}\mathbf{I}, \bar{\xi}\mathbf{I}$ and $\bar{\zeta}\mathbf{I}$, is known as a bi-isotropic chiral medium. Within the Rayleigh approximation, a nanospheroid can be modeled by the system of electric and magnetic dipoles placed in its geometric center. A 3D physical model for the rotational dynamics of a tri-axial nanospheroid with principal axes $(\mathbf{a}_x, \mathbf{a}_y, \mathbf{a}_z)$ (Fig.2), is considered.

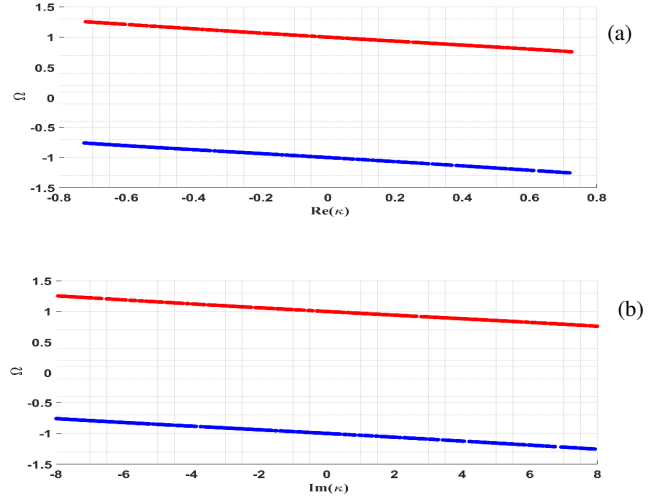


Fig.3. Domain of existence of equilibrium is given between the red and blue lines with the corresponding values of the nondimensional parameter Ω and real (a) and imaginary (b) parts of the chiral parameter $\kappa = \kappa_r(\text{Re}(\sqrt{\epsilon_r \mu_r}) + \text{Im}(\sqrt{\epsilon_r \mu_r})i)$, $-1 < \kappa_r < 1$.

The nanospheroid's permittivity is denoted by ϵ and is suspended in a fluid of permittivity ϵ_a and impedance Z_a . Relative permittivity and permeability of the fluid are defined as $\epsilon_r = \epsilon_a/\epsilon_0$ and $\mu_r = \mu_a/\mu_0 \approx 1$ (the subscript 0 represents the free space value). The particle is illuminated by a time-harmonic electromagnetic wave (EM) oscillating at the frequency ω (assuming time-dependence $e^{-i\omega t}$). Our model is generally formulated for a nanoellipsoid and degenerates to a nanospheroid by setting $a_y = a_z$ for the sake of simplification. A rotating frame of reference is attached to the ellipsoid mass center (body-fixed frame of reference) and the Eulerian angles (θ, ϕ, ψ) correspond to pitch, yaw and roll motions respectively.

The EM-field is linearly polarized with a rotating axis of polarization. Since the angle of polarization axis changes very slowly on the EM-field time scale, we can consider the time average of the torque \mathbf{T} over one optical cycle and apply the adiabatic approximation. The induced electric and magnetic dipole moments (\mathbf{p} and \mathbf{m}) can be accordingly expressed as [23]

$$\mathbf{p} = \bar{\alpha}_{ee}\mathbf{E} + \bar{\alpha}_{me}\mathbf{H} \quad (3a)$$

$$\mu_a \mathbf{m} = \bar{\alpha}_{em}\mathbf{E} + \bar{\alpha}_{mm}\mathbf{H} \quad (3b)$$

yielding the total torque acting on the nanospheroid. We will consider the case of Pasteur medium [14]. Furthermore, the

polarizability dyadics $\bar{\alpha}_{ee}, \bar{\alpha}_{em}, \bar{\alpha}_{me}, \bar{\alpha}_{mm}$ with $\bar{\alpha}_{em} = -\bar{\alpha}_{me}$ are given by

$$\alpha_{eej} = \Gamma_j \varepsilon_a [(\varepsilon - \varepsilon_a) [L_j \mu + (1 - L_j) \mu_a] - L_j \kappa^2 \mu_a \varepsilon_a] \quad (4a)$$

$$\alpha_{mmj} = \Gamma \mu_a [(\mu - \mu_a) [L_j \varepsilon + (1 - L_j) \varepsilon_a] - L_j \kappa^2 \mu_a \varepsilon_a] \quad (4b)$$

$$\alpha_{emj} = i \kappa \Gamma_j \mu_a \varepsilon_a \sqrt{\mu_a \varepsilon_a} \quad (4c)$$

where κ is chiral parameter, $j = x, y, z$, $\Gamma_j = 4\pi a_x a_y a_z / (3\Delta_j)$ and

$$\Delta_j = (L_j \mu + (1 - L_j) \mu_a) (L_j \varepsilon + (1 - L_j) \varepsilon_a) - L_j^2 \kappa^2 \mu_a \varepsilon_a \quad (4d)$$

The values L_j are the elements of diagonal depolarization tensor given by relations

$$L_j = 0.5 a_x a_y a_z \int_0^\infty \frac{1}{(s + a_j^2) R(s)} ds \quad (4e)$$

with $R(s) = \sqrt{(s + a_x^2)(s + a_y^2)(s + a_z^2)}$ and $L_x + L_y + L_z = 1$.

The depolarization coefficients expressed in terms of elliptic integrals [19]. The values ε, μ, κ (and therefore the elements of polarizability dyadic) are complex values.

III. THE DYNAMICAL SYSTEM

In the rotating frame of reference (X', Y', Z') the Newtonian equation of motion takes the form

$$\mathbf{L} = \langle \mathbf{T} \rangle - \mathbf{D} \quad (5)$$

where

$$\mathbf{L} = \mathbf{I} \dot{\tilde{\boldsymbol{\omega}}} + \tilde{\boldsymbol{\omega}} \times (\mathbf{I} \tilde{\boldsymbol{\omega}}) \approx 0 \quad (6a)$$

$$\langle \mathbf{T} \rangle = 0.5 [\text{Re}(\tilde{\mathbf{p}} \times \tilde{\mathbf{E}}^* + \mu_a \tilde{\mathbf{m}} \times \tilde{\mathbf{H}}^*) - k_0^3 / (12\pi) \text{Im}((1/\varepsilon_a) \tilde{\mathbf{p}}^* \times \tilde{\mathbf{p}} + \mu_a \tilde{\mathbf{m}}^* \times \tilde{\mathbf{m}})] \quad (6b)$$

$$\mathbf{D} = \mathbf{R} \tilde{\boldsymbol{\omega}} \quad (6c)$$

are the angular momentum, averaged EM torque and drag terms, respectively. The angular velocity of the particle in the rotating frame of reference $\tilde{\boldsymbol{\omega}}$ is a function of three Eulerian angles. For a chiral spheroid the nondimensional dynamical system, expressed in the Eulerian space, is given by

$$\begin{pmatrix} \Phi_\tau \\ \theta_\tau \\ \psi_\tau \end{pmatrix} = \begin{pmatrix} \gamma \sin^2 \psi - B_1 \cos \psi - \Omega \\ B_2 \\ B_3 - (\Phi_\tau + \Omega) \cos \theta \end{pmatrix} \quad (7)$$

where $\gamma = \tilde{E}^2 \alpha_{mez} / (\alpha R_x Z_a)$, B_1, B_2, B_3 are functions presented in appendix A and $\tau = \alpha t$ represents the normalized time. The proportionality factor α defined by (8), which is held constant through all simulations, is a functions of the EM amplitude, polarizabilities in two orthogonal directions and the angular drag coefficient R

$$\alpha = \tilde{E}^2 \text{Re}(\alpha_{eex} - \alpha_{eez}) / (4R) \quad (8)$$

with a dimension of 1/sec, \tilde{E} is a value of electric field and R is the angular drag coefficient in two perpendicular axes to

a_x ($R_z = R_y = R$). The non-dimensional angular frequency Ω is defined as

$$\Omega = 2\tilde{\Omega} / \alpha \quad (9)$$

where $\tilde{\Omega}$ denotes the dimensional angular frequency of the half wave plate. Note that the dynamical system (7) was obtained by approximating the second term in (6b) as zero (Appendix B). In addition, the non-dimensional transformation $\Phi = \phi - \Omega \tau$ is applied to the Eulerian angle ϕ which leads to the autonomous system (7) in terms of Φ . The index τ in (7) means a time derivative. The corresponding equilibrium points of the dynamical system are found by equating the left-hand side of (7) to zero and setting $\psi = 0$ ($\theta \in \mathbb{R}$) resulting at

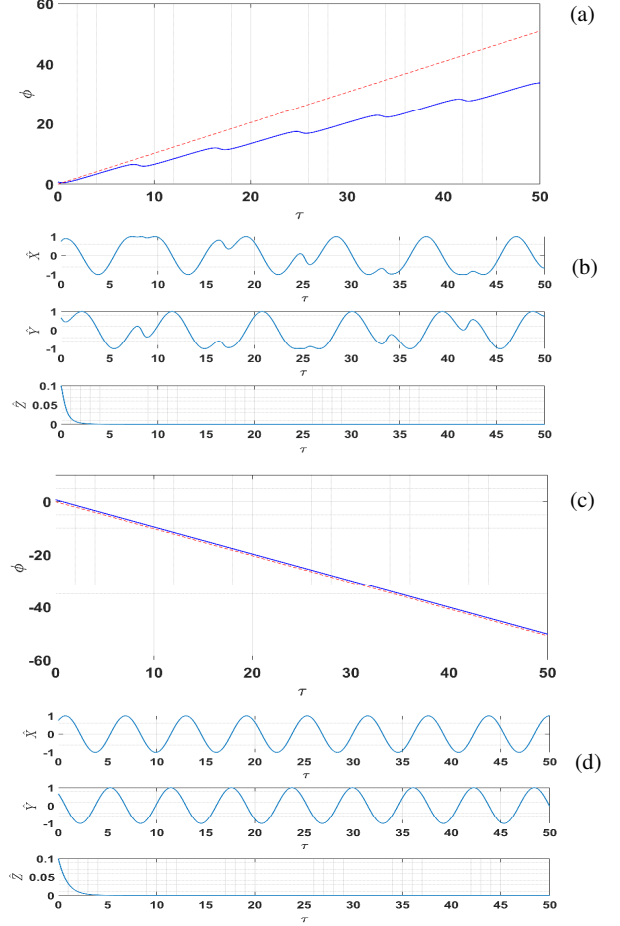


Fig.4 Time series of the dynamical system (7) for chiral parameter characterized by $\text{Re}(\kappa) = 0.1447$, $\text{Im}(\kappa) = 1.596$ and initial conditions $\Phi_0 = 0.73, \theta_0 = 1.57, \psi_0 = 0.1$ the value of proportionality parameter is $\alpha = 82.41$. In addition the value of the two nondimensional parameters are given by $\eta_1(\alpha_{eej}, \alpha_{mej}) = -0.048$ and $\eta_2(\alpha_{eej}, \alpha_{mmj}) = 1.341 \cdot 10^{-8}$ (Appendix A). (a),(b) correspond to $\tilde{\Omega} = 42 \text{ rad/sec}, \Omega = 1.02$ and (c),(d) correspond to $\tilde{\Omega} = -42 \text{ rad/sec}, \Omega = -1.02$. Dashed red line represents the nondimensional polarization angle $\Omega \tau$.

$$\begin{cases} -B_1 - \Omega = 0 \\ B_3 - \Omega \cos \theta = 0 \end{cases} \quad (10)$$

The system (10) renders the functions in (7) in terms of Ω . The values of the equilibrium angles $\phi_{1,2}^{\text{equil}}$ may be found from equation (10) as

$$\phi_1^{\text{equil}} = 0.5 \sin^{-1}[(\eta_1 - \Omega)/(1 + 0.5\eta_2)] \quad (11)$$

$$\phi_2^{\text{equil}} = \pi/2 - 0.5 \sin^{-1}[(\eta_1 - \Omega)/(1 + 0.5\eta_2)] \quad (12)$$

where η_1, η_2 two nondimensional parameters determined by polarizability tensor components. ($\eta_1 = \eta_1(\alpha_{\text{eej}}, \alpha_{\text{mej}})$ and $\eta_2 = \eta_2(\alpha_{\text{eej}}, \alpha_{\text{mmj}})$).

IV. OPTICAL TORQUE OF A SPHEROIDAL PARTICLE

In the limit of a non-chiral medium $\alpha_{\text{em}} = -\alpha_{\text{me}} = 0$, the system (7) reduces to the corresponding system obtained in [6]. The scenario of OT for the achiral case considered in [6], is controlled by the critical value of Ω for which $|\Omega_{\text{cr}}| = 1$. Values of $|\Omega| > 1$, correspond to the so-called non-linear motion, where the angle of the rod changes nonlinearly with time. This critical value separates two qualitatively different regimes of dynamics. For $|\Omega| < 1$ we get a phase-locked motion, for which the rod's motion exactly follows the rotation of the electric field polarization. It is also important to note, that a change in the sign of Ω generally leads to the inversion of rod rotation while keeping its dynamics (Fig.5).

We have performed here several simulations in different domains in the Ω, κ space (Fig.3), defined by the relations $\eta_1 - \Omega = \pm(1 + 0.5\eta_2)$ which correspond to the boundary for which the equilibrium (10) holds. It is worth mentioning that the value Ω depends on the chiral parameter which is usually a complex number. We have also considered a gold nanorod for two partial cases of real and imaginary chiral parameter (see Fig.3 a, b). The values of the chirality parameters are rather high. However, similar values of constitutive parameters have been reported in some other structures, such as DNA-Au, or chiral AU-colloids [21]. Future results can be also related to these types of artificial chiral structures. It is important to note, that the chosen chirality parameters satisfy the condition of $|\kappa| \ll \text{Im}(n)$ (n is a refractive index). This inequality guaranties that the rod is produced from a passive material [21]. Finally, the reader is recalled that for the effective implementation of OT, we need to have similar tensor values of the polarizabilities (i.e., different values for the longitudinal and transverse components) [6]. Such a property holds for a spheroid with an isotropic conductivity due to its non-symmetric configuration.

Our numerical simulations demonstrate (Fig.3) that for the chiral case one can readily separate out the phase-locked and the nonlinear regimes (with respect to Fig.3 b,d the set of coordinates $(\hat{X}, \hat{Y}, \hat{Z})$ correspond to the conventional set (X, Y, Z) via normalization by a_x , i.e., $\hat{X} = X/a_x, \hat{Y} = Y/a_x$ etc.). In a similar manner to the non-chiral case, the domain of the phase-locked motion, exists between the red and the blue lines depicted Fig. 3. However, in the chiral case this domain is not invariant with respect to the sign of the chirality.

As a result, the chirality of the rod dramatically changes the qualitative behavior of OT. For example, for

positive direction of rotation (Fig. 4c) the phase of the rod motion (blue line) follows exactly the rotation of the field polarization (red dashed line). Such dynamics corresponds to the monochromatic oscillations of the Cartesian coordinates (Fig 4b). By changing the direction of rotation (while keeping the value of its frequency), we obtain another scenario (Fig 4a). The rod decelerates in its rotation from that of the field polarization. Thereafter, it eventually stops and then starts to move in the opposite direction (this effect is named “flip-back” in [6]). After some time, the rod regains its initial direction of motion. Thereby, the dynamics of the rod corresponds a periodic chain of “flip-backs” strokes.

However, in contrast with [6], the OT dynamics in the chiral case, depends on the direction of rotation of the EM-field polarization axis. The OT dynamics is also different for a right-hand chirality and a left-hand chirality and depends on the chirality value. At the Fig. 5 it is shown the dynamics of the structure with the opposite sign of chirality value. One can see again the phase-locked and the nonlinear regimes with the same dynamics subject to the direction of rotation. However, every of these regimes exist for the opposite directions of rotation.

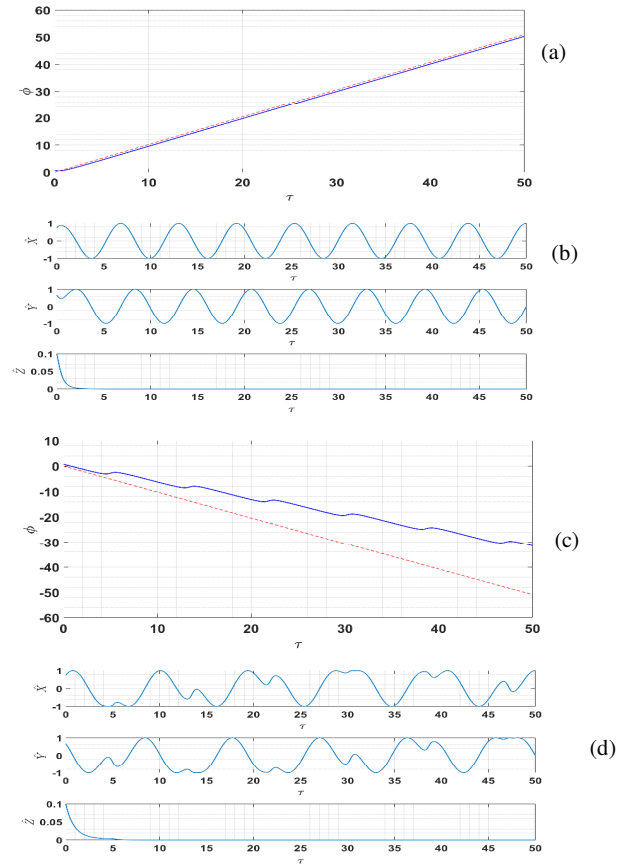


Fig.5 Time series of the dynamical system (7) from initial conditions $\Phi_0 = 0.73, \theta_0 = 1.57, \psi_0 = 0.1$ and parameters $\eta_1 = 0.048, \eta_2 = 1.341 \cdot 10^{-8}, \alpha = 82.419, \text{Re}(\kappa) = 0.1447, \text{Im}(\kappa) = -1.0596$ (a),(b) correspond to $\tilde{\Omega} = 42 \text{ rad/sec}, \Omega = 1.02$ and (c),(d) correspond to $\tilde{\Omega} = -42 \text{ rad/sec}, \Omega = -1.02$.

Fig. 6 shows the dynamics of achiral spheroid. In this case, we see identical non-linear dynamics for both directions of rotation. In contrast with the non-chiral case [6], such dynamics with the same angular velocity is reachable only in one direction of rotation (positive value Ω). Changing the direction of Ω leads to a breakdown of the nonlinear regime and a transition to the phase-locked regime. Due to the special chiral asymmetry, the phase-locked dynamics is reachable for a dual system (i.e., changing sign of chirality).

V. CONCLUSION AND OUTLOOK

In this paper we have predicted the novel mechanism of OT of small spheroidal particles made from a chiral material. The OT is considered as a linearly polarized EM-field with rotating polarization axis.

The dynamical equations and the conditions of stationary state are formulated and numerically simulated. The results of our analysis demonstrate the qualitative influence of the chirality on the OT.

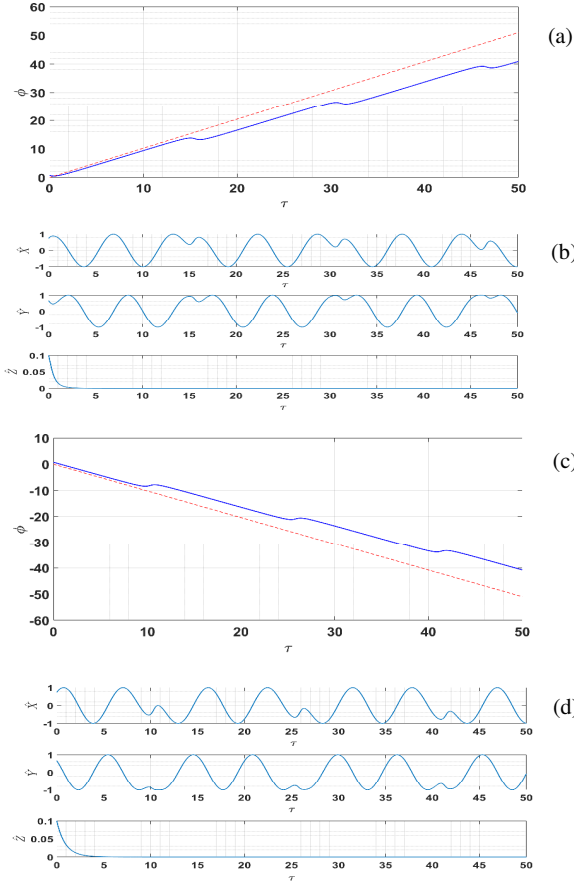


Fig.6 Time series of the dynamical system (7) from initial conditions $\Phi_0 = 0.73, \theta_0 = 1.57, \psi_0 = 0.1$ and parameters $\eta_1 = \eta_2 = 0, \alpha = 82.419, \text{Re}(\kappa) = \text{Im}(\kappa) = 0$ (a),(b) correspond to $\tilde{\Omega} = 42 \text{ rad/sec}, \Omega = 1.02$ and (c),(d) correspond to $\tilde{\Omega} = -42 \text{ rad/sec}, \Omega = -1.02$.

In a similar manner to the non-chiral case [6], we find that two regimes of OT dynamics exist: phase-locked motion and non-linear motion. This effect may be found useful in different applications such as: i) measurements of

chiral parameters; ii) optical enantio-sorting of chiral objects iii) design of optical driven micro-machines; etc.

A similar effect also exists in other types of helix-like structures, such as chiral carbon nanotubes, plasmonic nanohelices, DNA-Au, or chiral AU-colloids. Such objects may be described by the dipole approximation, but the model of chiral dielectric is invalid for the calculation of their polarizability. Among the many remarkable properties of chiral objects, we mention here the internal EM-resonance (“antenna resonance”), which seems to be an effective manifestation tool also in optomechanics. This is certainly one of the promising directions for future research activity.

APPENDIX A

For the functions $\mathcal{B}_1, \mathcal{B}_2, \mathcal{B}_3$ in equation (7) we have

$$\mathcal{B}_1 = \sigma_1(\eta_2 \cos \Phi - \eta_1 \sin \Phi) + \sigma_2(2 \sin \Phi - \eta_1 \cos \Phi) \quad (\text{A1})$$

$$\mathcal{B}_2 = \sin \psi \sin \theta (\mathcal{B}_1 + \gamma \cos \psi) \quad (\text{A2})$$

$$\mathcal{B}_3 = \sigma_1(\sigma_4 \eta_1 + \sigma_3 \eta_2) - \sigma_2(2\sigma_4 + \sigma_3 \eta_1) \quad (\text{A3})$$

where $\eta_1 = \delta_4 + \delta_2, \eta_2 = \delta_1 - \delta_3$. The coefficients $\delta_u, u = 1, 2, 3, 4$ are functions of dyadic polarizabilities, elements of which are given by

$$\delta_1 = 2 \text{Re}(\alpha_{mmz}) / [Z_a^2 \text{Re}(\alpha_{eex} - \alpha_{eez})] \quad (\text{A4})$$

$$\delta_2 = 2 \text{Re}(\alpha_{mez}) / [Z_a \text{Re}(\alpha_{eex} - \alpha_{eez})] \quad (\text{A5})$$

$$\delta_3 = 2 \text{Re}(\alpha_{mmx}) / [Z_a^2 \text{Re}(\alpha_{eex} - \alpha_{eez})] \quad (\text{A6})$$

$$\delta_4 = 2 \text{Re}(\alpha_{mex}) / [Z_a \text{Re}(\alpha_{eex} - \alpha_{eez})] \quad (\text{A7})$$

where Z_a is the impedance of the surrounding achiral fluid. The values $\sigma_i, i = 1, 2, 3, 4$ are the functions of Eulerian angles and are given by

$$\sigma_1 = \cos \psi \sin \Phi + \sin \psi \cos \theta \cos \Phi \quad (\text{A8})$$

$$\sigma_2 = \cos \psi \cos \Phi - \sin \psi \cos \theta \sin \Phi \quad (\text{A9})$$

$$\sigma_3 = \sin \psi \sin \Phi - \cos \psi \cos \theta \cos \Phi \quad (\text{A10})$$

$$\sigma_4 = \sin \psi \cos \Phi + \cos \psi \cos \theta \sin \Phi \quad (\text{A11})$$

APPENDIX B

Let the magnitude of the incident EM field defined as

$$\tilde{\mathbf{E}} = |\mathbf{E}|, \tilde{\mathbf{H}} = |\mathbf{H}| \quad (\text{B1})$$

in addition, we define the following non-dimensional variables

$$\mathbf{E}_0 = \mathbf{E} / \tilde{\mathbf{E}}, \mathbf{H}_0 = \mathbf{H} / \tilde{\mathbf{H}}, \mathbf{p}_0 = \mathbf{p} / (\epsilon_a a_x^3 \tilde{\mathbf{E}})$$

$$\mathbf{m}_0 = \mathbf{m} / (a_x^3 \tilde{\mathbf{H}}), k_0 = a_x k_a, \langle \mathbf{T} \rangle_0 = \langle \mathbf{T} \rangle / (\epsilon_a a_x^3 \tilde{\mathbf{E}}^2) \quad (\text{B2})$$

where a_x is half of the length of the major axis of the spheroid. The nondimensional form of (6b) reads

$$\langle T \rangle_0 = 0.5 [\text{Re}(\mathbf{p}_0 \times \mathbf{E}_0^* + \mathbf{m}_0 \times \mathbf{H}_0^*) - k_0^3 / (12\pi) \text{Im}((\mathbf{p}_0^* \times \mathbf{p}_0) + (\mathbf{m}_0^* \times \mathbf{m}_0))] \quad (\text{B3})$$

for a nonmagnetic achiral particle, the relation (B3) degenerates to

$$\langle T \rangle_0 = 0.5 \left[\text{Re}(\mathbf{p}_0 \times \mathbf{E}_0^*) + \frac{k_0^3}{6\pi} \text{Im}((\mathbf{p}_0 \times \mathbf{p}_0^*)) \right] \quad (\text{B4})$$

in the Rayleigh regime the radiative correction to the polarizability is given by [24]

$$\alpha_{eej} = \tilde{\alpha}_{eej} / [1 - i\tilde{\alpha}_{ee} k_a^3 / (6\pi)] \quad (\text{B5})$$

where $\tilde{\alpha}_{eej}$ stands for the polarizability at the electrostatic limit with $j = x, y, z$. In terms of the non-dimensional polarizability α_{eej}^0 we have

$$\alpha_{eej}^0 = \tilde{\alpha}_{eej}^0 / [1 - i\tilde{\alpha}_{ee}^0 k_0^3 / (6\pi)] \quad (\text{B6})$$

where $\tilde{\alpha}_{eej}^0 = \tilde{\alpha}_{eej} / (\epsilon_a a_x^3)$ is the nondimensional static polarizability. Furthermore

$$\alpha_{eej}^0 = \frac{\tilde{\alpha}_{eej}^0}{1 - i\tilde{\alpha}_{eej}^0 k_0^3 / (6\pi)} \frac{1 + i\tilde{\alpha}_{eej}^{0*} k_0^3 / (6\pi)}{1 + i\tilde{\alpha}_{eej}^{0*} k_0^3 / (6\pi)} \quad (\text{B7})$$

and after neglecting sixth degree terms

$$\alpha_{eej}^0 \approx \tilde{\alpha}_{eej}^0 + i|\tilde{\alpha}_{eej}^0|^2 k_0^3 / (6\pi) \quad (\text{B8})$$

The averaged torque for the nonmagnetic case is then together with (B8) becomes

$$\langle T \rangle_{0j} = 0.5 [\text{Re}(\mathbf{p}_0 \times \mathbf{E}_0^*)_j] = 0.5 \text{Re}(\alpha_{eej}^0 (\mathbf{E}_0 \times \mathbf{E}_0^*)_j) \quad (\text{B9})$$

$$\langle T \rangle_{0j} = 0.5 \left[\text{Re} \left(\left\{ \tilde{\alpha}_{eej}^0 + i|\tilde{\alpha}_{eej}^0|^2 k_0^3 / (6\pi) \right\} (\mathbf{E}_0 \times \mathbf{E}_0^*)_j \right) \right] \quad (\text{B10})$$

$$\langle T \rangle_{0j} = 0.5 [\text{Re}(\mathbf{p}_0 \times \mathbf{E}_0^*)_j] + k_0^3 / (12\pi) \text{Im}(\mathbf{p}_0 \times \mathbf{p}_0^*)_j \quad (\text{B11})$$

hence, adding the second term in (B4) is equivalent to replacing $\tilde{\alpha}_{eej}$ by α_{eej} and computing $\langle T \rangle_{0j}$ only by the first cross product. In the Rayleigh regime we take $\alpha_{eej} \approx \tilde{\alpha}_{eej}$.

REFERENCES

- [1] Y. Geng, J. Tan, Y. Cao, Y. Zhao, Z. Liu, W. Ding, "Giant and Tunable Optical Torque for Micro-Motors by Increased Force Arm and Resonantly Enhanced Force", *Scientific Reports*, 2018.
- [2] M. Gudipati, J. D'Souza, J. Dharmadhikari, A. Dharmadhikari, B. Rao, D. Mathur, "Optically-Controllable," Micron-Sized Motor Based on Live Cells", *Optics Express* 13, 1555–1560, 2005.
- [3] M. G. L. Van Den Heuvel, C. Dekker, "Motor Proteins at Work for Nanotechnology" *Science*, 317, 333–336, 2007.
- [4] S. Kuhn, A. Kosloff, B. A. Stickler, F. Patolsky, K. Hornberger, M. Arndt, J. Millen, "Full Rotational Control of Levitated Silicon Nanorods", *Optica*, 356–360, 2017.
- [5] S. H. Simpson, S. Hanna, "Holographic Optical Trapping of Microrods and Nanowires" *Journal of the Optical Society of America A, Optics Image Science and Vision*, 27, 1255–1264, 2010.
- [6] W. A. Shelton, Bonin K. D., Walker, T. G., "Nonlinear Motion of Optically Torqued Nanorods", *Phys. Rev. E*, 71, 8, 2005.
- [7] P. H. Jones, O. M. Marago, G. Volpe, "Optical Tweezers-Principles and Applications", Cambridge University Press, 2015
- [8] M. Khan, A. K. Sood, F. L. Deepak, C. N. R. Rao, "Nanorotors using Asymmetric Inorganic Nanorods in an Optical Trap", *Nanotechnology* 17, S287–S290, 2006.
- [9] K. Ding, J. Ng, L. Zhou, C. T. Chan, "Realization of Optical Pulling Forces Using Chirality", *Phys. Rev. A*, 89, 063825, 2014.
- [10] D. Hakobyan, E. Brasselet, "Left-Handed Optical Radiation Torque", *Nature Photonics*, 610–614, 142, 2014.
- [11] Wang, S. B., Chan, C. T., "Lateral optical force on chiral particles near a surface", *Nature Communication*. 5, 4307, 2014.
- [12] A. Rahimzadegan, M. Fruhnert, R. Alaei, I. Fernandez Corbaton, and C. Rockstuhl, "Optical force and torque on dipolar dual chiral particles", *Phys. Rev. B*, 94, 125123, 2016.
- [13] M. N. Vesperinas, "Optical Torque on Small Bi Isotropic Particles", Vol. 40, No. 13, *Optics Letters*, 2015.
- [14] C. Genet, "Chiral Light-Chiral Matter Interactions: An Optical Force Perspective", *ACS Photonics*, 9, 2, 319–332 Publication Date: January 26, 2022
- [15] C. Caloz, A. Sihvola, "Electromagnetic Chirality", *IEEE Antennas & Propagation Magazine*, 1045–9243, 2020.
- [16] J. Mun, M. Kim, Y. Yang, T. Badloe, J. Ni, Y. Chen, C. W. Qiu, J. Rho, "Electromagnetic Chirality: From Fundamentals to Nontraditional Chiroptical Phenomena", *Light: Science & Applications*, 2020.
- [17] X. Zhang, Z. Yu, C. Wang, D. Zarrouk, J. W. T. Seo, J. C. Cheng, D. Buchan, K. Takei, Y. Zhao, J. W. Ager, J. Zhang, M. Hettick, M. C. Hersam, A. P. Pisano, R. S. Fearing, A. Javey, "Photo actuators and Motors Based On Carbon Nanotubes with Selective Chirality Distributions", *Nature Communications*, 2013.
- [18] W. Wu, M. Pauly, "Chiral plasmonic nanostructures: recent advances in their synthesis and applications", *Mater. Adv.*, 3, 186, 2022.
- [19] Y. Wang, J. Xu, Y. Wang, H. Chen, "Emerging Chirality in Nanoscience", *Chem. Soc. Rev.*, 42, 2930, 2013.
- [20] A. Lakhtakia, "Polarizability Dyadic of Small Chiral Ellipsoids", *Chemical Physics Letters*, Vol. 174, No. 6, 1990.
- [21] A. Canaguier-Durand, C. Genet, "Chiral Route to Pulling Optical Forces and Left-Handed Optical Torques", *Phys. Rev. A*, 92, 043823, 2015.
- [22] C. F. Bohren, D. R. Huffman, "Absorption and Scattering of Light by Small Particles", Wiley, 1983.
- [23] M. Schaferling, "Chiral Nanophotonics-Chiral Optical properties of plasmonic systems", *Springer*, 2017
- [24] A. H. Sihvola, "Electromagnetic modeling of Bi-isotropic Media, Progress in Electromagnetics research", *PIER* 9, 45–86, 1994.
- [25] S. Albaladejo, R. Gómez-Medina, L. S. Froufe-Pérez, H. Marinchio, R. Carminati, J. F. Torrado, G. Armelles, A. García-Martín, J. J. Sáenz, "Radiative corrections to the polarizability tensor of an electrically small anisotropic dielectric particle", *Optics Express*, Vol. 18, No. 4, 2010.